

Electronic Supporting Information

pH-induced reorientation of cytochrome *c* on silica nanoparticles

Jens Meissner¹, Yao Wu², Jacques Jestin³, William A. Shelton^{2,4}, Gerhard H. Findenegg^{1,*} and Bhuvnesh Bharti^{2,*}

¹*Stranski Laboratory of Physical and Theoretical Chemistry, Technical University Berlin, 10623 Berlin, Germany*

²*Cain Department of Chemical Engineering, Louisiana State University, Baton Rouge, LA 70803, USA*

³*Laboratoire Léon Brillouin, CEA Saclay 91191 Gif-sur-Yvette Cedex, France*

⁴*Center for Computation and Technology, Louisiana State University, Baton Rouge, LA 70803, USA*

E-mail: findenegg@chem.tu-berlin.de; bbharti@lsu.edu

Table of Contents

I.	Characterization of silica particles and cytochrome <i>c</i>	S1
II.	Fitting of SANS data with the RB model	S3
III.	Adsorption isotherms and calculation of expected surface coverage	S9
IV.	MD simulation details	S10
V.	Instrumental details SANS	S13

I. Characterization of silica particles and cytochrome c

The shape and size of the protein in the absence of silica nanoparticles was determined by SANS. SANS profiles in D₂O were measured in the pH range 3 - 10 and were fitted with the form factor of randomly oriented oblate ellipsoids. The fit of the SANS data and the resulting values of the equatorial (D_p^{eq}) and axial (D_p^{ax}) diameter of cytochrome c are displayed in Figure S1. We find that the two diameters remains constant within the experimental error margin over the studied pH range, with $D_p^{\text{eq}} = 3.7 \pm 0.2$ nm and $D_p^{\text{ax}} = 2.1 \pm 0.2$ nm.

The size and polydispersity of the silica nanoparticles, and their volume fraction in the dispersions in D₂O was determined by fitting the SANS profiles of the silica dispersions in the absence of protein with the form factor of spheres with a log-normal size distribution (Figure S2). Results are summarized in Table S1.

Table S1. Mean diameter D_s and polydispersity of the three types of silica nanoparticles used in this study, and their volume in the dispersion determined by fitting experimental SANS profiles of the silica nanoparticle dispersions.

Sample	Mean diameter D_s /nm	Polydispersity	Volume fraction
SiNP7	7	0.17	0.0051
SiNP13	13	0.14	0.0051
SiNP41	41	0.13	0.0164

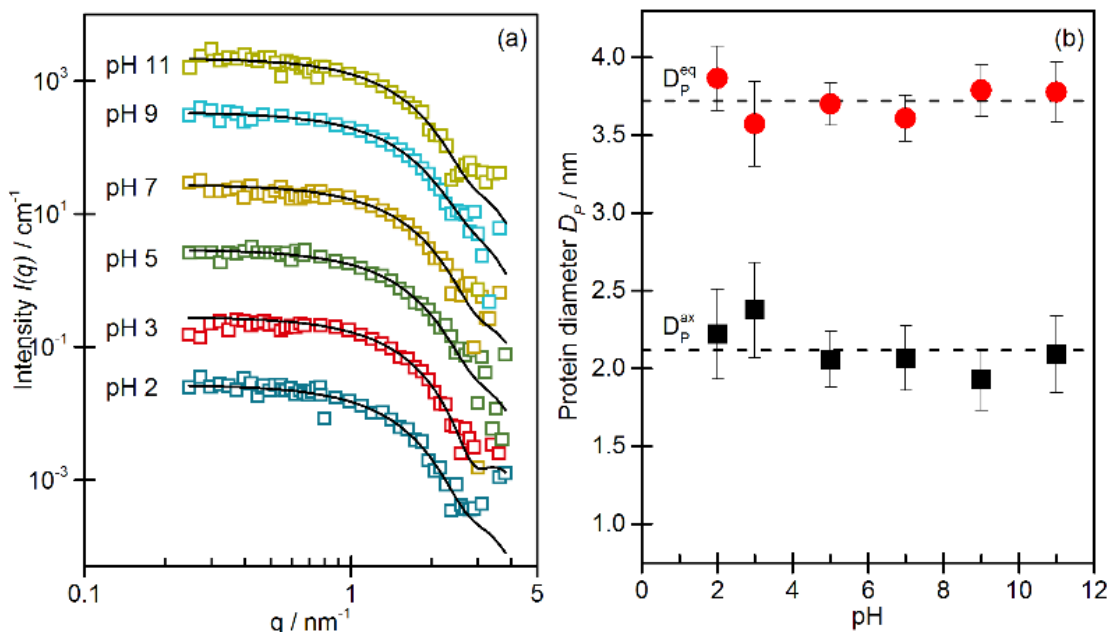


Figure S1. (a) Small angle neutron scattering intensity profiles $I(q)$ for cytochrome c in D_2O in the absence of nanoparticles at different bulk pH values as indicated in the graph. Solid lines represent fits with a form factor model accounting for non-interacting ellipsoid. The curves are shifted by a constant factor of 10 for better visualization. (b) The resulting fit values for the equatorial and axial axis of the ellipsoidal model for different pH conditions. The dashed lines represent the mean value of the displayed data points.

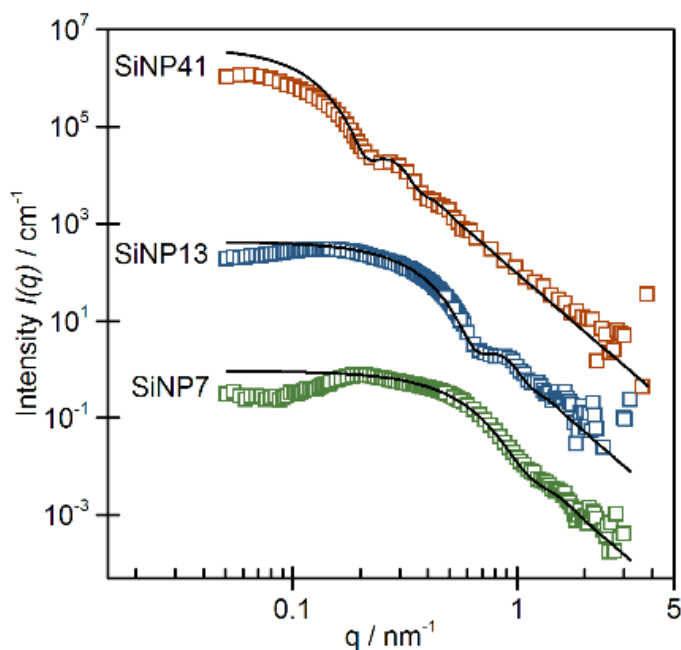


Figure S2. Small angle neutron scattering intensity profiles $I(q)$ for SiNP7, SiNP13 and SiNP41 particles in D_2O in the absence of cytochrome c at pH 8.3. Solid lines represent fits with a form factor model accounting for non-interacting solid spheres. Tabulated fit parameter are given in Table S1. The curves are shifted by a constant factor of 100 for better visualization.

The present study is aiming at the spatial orientation of cytochrome *c* molecules at silica nanoparticles. To access this information, scattering originating from cytochrome *c* adsorbed at silica nanoparticles was studied. Neutron scattering in D₂O is a promising method for this purpose because the scattering contrast of proteins and particles to D₂O is high (i.e., their scattering length densities are very different from D₂O). In order to minimize incoherent scattering from protons (H atoms) the nanoparticles were synthesized directly in D₂O. SANS experiments were performed on 1 wt% silica particle dispersions (3.2 wt% for SiNP41) containing a fixed amount of cytochrome *c*. The amount of cytochrome *c* was chosen such that at pH 8.3 essentially all protein was adsorbed on the particles and no free protein remained in solution. The pH of the dispersion was varied in the range 2-11 by the addition of small amounts of 0.1N HCl or 0.1N NaOH. The resulting SANS profiles were then analyzed using the SasView software package.

II. Fitting of SANS data with the RB model

The SANS profile $I(q)$ of a dispersion is obtained by radially averaging the corresponding 2D scattering pattern. It is related to the shape, size, concentration, composition and spatial distribution of the scattering objects as¹

$$I(q) = N\Delta\rho^2 P(q)S(q) \quad (1)$$

where N is the number of scattering objects, $\Delta\rho$ the scattering length density contrast of the particles against the matrix (here D₂O), and q is the scattering vector related to neutron wavelength (λ) and angle of scattering (θ) as $q = (4\pi/\lambda) \sin(\theta/2)$. In eq. 1, the form factor $P(q)$ is a function of particle shape and size, and the structure factor $S(q)$ is the measure of spatial correlation between these particles. For particle dispersions the characteristic interparticle separation (center-to-center distance) is always larger than the particle diameter, hence $S(q)$ selectively affects $I(q)$ at low

scattering vectors q , and $P(q)$ selectively influences the scattering intensity at higher q . In this work we study the assembly of protein molecules on the individual silica nanoparticles. This information is contained in the form factor of the silica-protein composite. Accordingly, we focus on the model dependent analysis of the form factor $P(q)$ in a q range in which the structure factor does not contribute ($S(q) = 1$).

Accessing a detailed picture of nanoscale entities by small-angle scattering relies on an appropriate form factor model that represents the geometrical features of the entity. In Figure 1 of the paper three different form factor models, representing three possible scenarios for the assembly of cytochrome *c* and silica nanoparticles, are compared with an experimental scattering profile. These are: (a) A mixture of non-interacting spheres and ellipsoids, to represent silica nanoparticles and nonadsorbed protein; (b) particles with a uniform shell, to represent protein forming a uniform shell at the particles; and (c) particles decorated with individual spherical objects, to represent discrete protein molecules adsorbed at the silica particles. The form factor model of ‘raspberry-like’ particles by Larson-Smith et al.² was used here (see below). The parameter values used to simulate the three scattering profiles are given in Table S2.

Table S2. Model parameters of the simulations in Figure 1. Simulations were based on the assumption of (a) non-interacting SiNP and cytochrome *c* particles; (b) a core-shell particle consisting of a central silica sphere and a uniform shell of cytochrome *c* molecules; (c) a central silica sphere decorated with individual cytochrome *c* molecules.

Parameter	(a) Independent spheres and ellipsoids	(b) Spherical core-shell particles	(c) ‘Raspberry-like’ particles
$D_{\text{SiNP}}/\text{nm}$	7.2	7.2	7.2
$\text{PDI}_{\text{SiNP}}/-$	0.171	0.171	0.171
$\varphi_{\text{SiNP}}/-$	0.0050	0.0231) ¹	0.0050
$D_{\text{protein}}/\text{nm}$	$D_{\text{p}}^{\text{ax}} = 2.4$ $D_{\text{p}}^{\text{eq}} = 3.6$	2.4) ²	2.4/3.6
$\varphi_{\text{protein}}/-$	0.0041	0.0041	0.0041
$SLD_{\text{SiNP}}/\text{\AA}^2$	$3.48 \cdot 10^{-6}$	$3.48 \cdot 10^{-6}$	$3.48 \cdot 10^{-6}$
$SLD_{\text{protein}}/\text{\AA}^2$	$3.07 \cdot 10^{-6}$	$5.64 \cdot 10^{-6}$	$3.07 \cdot 10^{-6}$
$SLD_{\text{solvent}}/\text{\AA}^2$	$6.09 \cdot 10^{-6}$	$6.09 \cdot 10^{-6}$	$6.09 \cdot 10^{-6}$
$\phi_{\text{p}}^{\text{a}}/-$) ³	-) ⁴	-) ⁴	0.54/0.35

)¹ volume fraction of the complete core-shell particle;)² corresponds to the shell thickness in the core-shell model;

)³ fraction of SiNP surface covered with protein was calculated as $\phi_{\text{p}}^{\text{a}} = (N_{\text{protein}}A_{\text{protein}})/A_{\text{SiNP}}$;)⁴ this parameter is not necessary in this model

The model of ‘raspberry-like’ particles (RB-model) reported by Larson-Smith et al.² was originally developed to represent nanoparticles attached to oil droplets in Pickering emulsions. It assumes a random distribution of small spherical particles attached to each of the oil droplets and it allows for a fraction of particles remaining nonadsorbed. Using the notation of the present paper, i.e., replacing the oil by silica particles (subscript s), and the small particles by the protein (subscript p), the scattering intensity is given by (cf. Eq. 12 of ref. 2):

$$I(q) = (\phi_{\text{s}}V_{\text{s}}\Delta\rho_{\text{s}}^2 + \phi_{\text{p}}\phi_{\text{p}}^{\text{a}}V_{\text{p}}\Delta\rho_{\text{p}}^2N_{\text{p}})P_{\text{RB}}(q) + \phi_{\text{p}}(1 - \phi_{\text{p}}^{\text{a}})V_{\text{p}}\Delta\rho_{\text{p}}^2P_{\text{P}}(q) \quad (2)$$

where the first term contains the form factor $P_{RB}(q)$ of the raspberry-like particles and represents scattering of these composite particles, the second term contains the form factor $P_p(q)$ of the free protein and represents its contribution to the scattering of the dispersion. In eq. 2, ϕ_s and ϕ_p are the volume fractions of silica particles and protein in the dispersion, ϕ_p^a is the fraction of protein adsorbed at the silica particles, V_s and V_p represent, respectively, the volume of a silica particle and a protein molecule, $\Delta\rho_s = |\rho_{\text{silica}} - \rho_{\text{D}_2\text{O}}|$ and $\Delta\rho_p = |\rho_{\text{protein}} - \rho_{\text{D}_2\text{O}}|$ are the scattering length density contrasts of silica and protein against the dispersing medium (D_2O). Because in the present case the adsorbed protein is just touching the silica particles, we apply the model with $\delta = 1$ (cf. Fig. 1 of ref. 2). The number of protein molecules at the surface of a single silica particle, N_p , which appears in the first term of eq. 2, is calculated as a function of χ , the fraction of surface area of the particle covered (or “shadowed”) by protein²

$$\chi = \frac{4\phi_p\phi_p^a(D_s+D_p)}{\phi_s D_p} \quad (3)$$

where D_s and D_p are the diameters of the spherical silica particles and protein. For the number of protein molecules per silica particle this yields

$$N_p = \frac{\phi_p\phi_p^a V_s}{\phi_s V_p} = \chi \frac{4D_p}{(D_s+D_p)} \frac{V_s}{V_p} \quad (4)$$

The form factor of the raspberry-like particles can be calculated by solving Debye equations and is given by²

$$P_{RB} = \frac{1}{M^2} [\Delta\rho_s^2 V_s^2 \Psi_s^2 + N_p \Delta\rho_p^2 V_p^2 \Psi_p^2 + N_p(N_p - 1) \Delta\rho_p^2 V_p^2 S_{pp} + 2N_p \Delta\rho_s \Delta\rho_p V_s V_p S_{sp}] \quad (5)$$

where

$$M = \Delta\rho_s V_s + N_p \Delta\rho_p V_p$$

$$\Psi_s = \frac{3[\sin(qR_s) - qR_s \cos(qR_s)]}{(qR_s)^3}$$

$$\Psi_p = \frac{3[\sin(qR_p) - qR_p \cos(qR_p)]}{(qR_p)^3}$$

$$S_{pp} = \Psi_p^2 \left[\frac{\sin(q(D_s + D_p))}{q(D_s + D_p)} \right]^2$$

$$S_{sp} = \Psi_s \Psi_p \frac{\sin(q(D_s + D_p))}{q(D_s + D_p)}$$

In this experimental study, all parameters of eq. 2 are known except for the cytochrome *c* diameter (D_p) and the fractional surface coverage of the central particle (ϕ_p^a). Hence, the experimental SANS profiles of cytochrome *c* bound to silica nanoparticles can be fitted using the RB-model with only D_p and ϕ_p^a as free parameters.

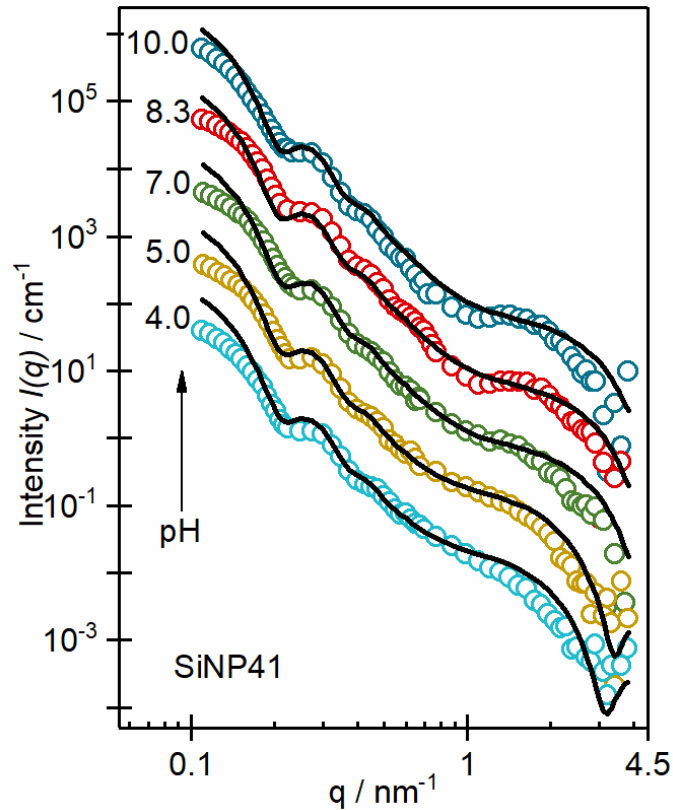


Figure S3. Small angle neutron scattering intensity profiles $I(q)$ for SiNP41 particles in D_2O with a fixed amount of cytochrome *c* at different bulk pH values as indicated in the graph. The curves are shifted by a constant factor of 10 for better visualization.

Table S3. Values of the fixed general parameters used for the RB model fitting of the SANS intensity curves in Figure 2 and Figure S3: diameter of the silica particle D_{SiNP} , its polydispersity s_{SiNP} , volume fractions of silica φ_{SiNP} and cytochrome *c* φ_{protein} , scattering length densities SLD of silica, solvent and cytochrome *c*. Parameter δ accounts for penetration of the central particle by the outer particles ($\delta = 1$ corresponds to no penetration; cf. Fig. 1 of ref. 2))

	SiNP7	SiNP13	SiNP41
$D_{\text{SiNP}}/\text{nm}$	7.2	12.9	40.8
$s_{\text{SiNP}}/-$	0.17	0.14	0.13
$\varphi_{\text{SiNP}}/-$	0.0051	0.0051	0.0164
$\varphi_{\text{protein}}/-$	0.0041	0.0012	0.0032
$SLD_{\text{SiNP}}/\text{\AA}^2$		$3.48 \cdot 10^{-6}$	
$SLD_{\text{solvent}}/\text{\AA}^2$		$6.09 \cdot 10^{-6}$	
$SLD_{\text{protein}}/\text{\AA}^2$		$2.90 \cdot 10^{-6}$	
$\delta/-$		1	

Table S4. Best fit values of the open parameters D_p and χ of the RB model fitting of the SANS intensity curves Figure 2 and Figure S3 at different pH. D_p is the effective diameter of the adsorbed protein molecule, χ the fraction of the nanoparticle surface covered with protein.

SiNP7			SiNP13			SiNP41		
pH	$\frac{D_p}{\text{nm}}$	χ	pH	$\frac{D_p}{\text{nm}}$	χ	pH	$\frac{D_p}{\text{nm}}$	χ
3.0	3.4	0.14	4.0	3.2	0.03	2.3	2.9	0.40
4.5	3.4	0.28	5.0	3.4	0.06	3.3	2.7	0.47
6.5	3.1	0.40	7.0	2.2	0.41	5.3	2.1	0.49
8.3	2.4	0.55	8.3	2.2	0.47	7.3	2.0	0.90
9.6	2.6	0.54	10.0	2.5	0.32	8.3	2.0	0.70
						11.3	2.0	0.85

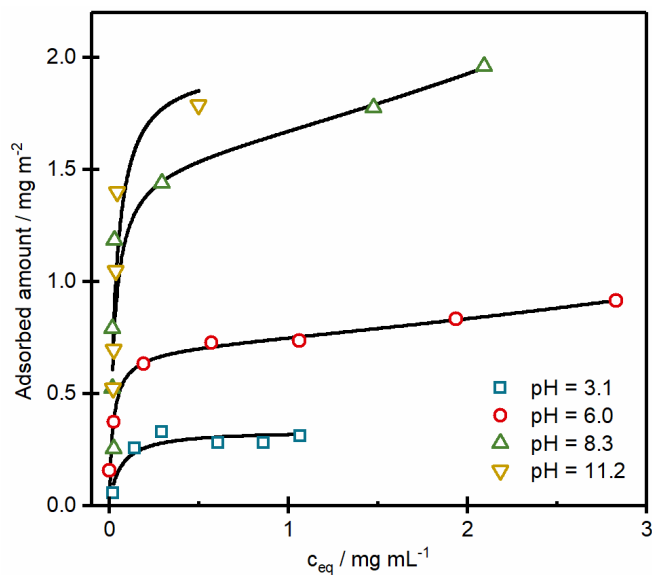


Figure S4. Adsorption isotherms for cytochrome *c* on silica nanoparticles (Ludox TMA, $D_{SiNP} = 27$ nm) at different pH conditions as indicated. Solid lines are fits with the GAB model introduced in Part III. Best fit values of the parameters are given in Table S4.

cytochrome c in the SANS sample it is possible to calculate the adsorbed amount. Fractional surface coverages are calculated based on the assumption of a side-on footprint of the cytochrome c molecule. Figure 3 of main paper compares the fractional surface coverage for the SANS samples as derived from the fit of the RB model with the surface coverage as obtained from the protein adsorption measurements with the GAB adsorption isotherm equation. For SiNP7 the results obtained by the two methods are in excellent agreement. For SiNP13 and SiNP41 reasonable agreement is found, except for some unsystematic deviations at low pH.

Table S5. Best fit values of the GAB parameters for the experimental adsorption isotherms in Figure S-4.

pH	K_S mL/mg	K_L mL/mg	Γ_m mg/m ²
3.1	16.3	0.00	0.34
6.0	45.1	0.09	0.70
8.3	36.4	0.11	1.52
11.2	28.0	0.00	1.98

IV. MD simulation details

The CHARMM potential energy E for silica⁴ shown in eq. 6 contains 12-6 and 9-6 Lennard-Jones potentials for repulsive and dispersive van-der-Waals interactions, respectively, a Coulomb potential for electrostatic interaction, and harmonic potentials for bond stretching and angle bending. The non-bonded CHARMM parameters for silica and the silica surface are summarized in Table S6. 2GIW.pdb⁵ from the protein database was used as the starting cytochrome c structure. Six simulation systems were prepared for different silica surface of pH 3-9. The protein was initially neutralized with NaCl solution at ionic strength of 2×10^{-2} M, a rectangular water box (TIP3P model) with dimension of $101 \text{ \AA} \times 105 \text{ \AA}$ (silica surface dimension) $\times 85 \text{ \AA}$ (protein/water space) was created and finally the silica surface was merged to the system.

$$E = \sum_{ij, \text{bonded}} k_{r,ij} (r_{ij} - r_{0,ij})^2 + \sum_{ijk, \text{bonded}} k_{ijk} (\theta_{ijk} - \theta_{0,ijk})^2 + \sum_{ij, \text{nonbonded}} \epsilon_{ij} \left[\left(\frac{\sigma_{ij}}{r_{ij}} \right)^{12} - 2 \left(\frac{\sigma_{ij}}{r_{ij}} \right)^6 \right] + \frac{1}{4\pi\epsilon_0} \sum_{ij, \text{nonbonded}} \frac{q_i q_j}{r_{ij}} \quad (6)$$

Table S6. Nonbonded Parameters for Silica and Silica Surfaces

atom	Charge (e)	12-6 LJ CHARMM	
		σ_{ii} (Å)	${}^b r_{ii}$ (kcal/mol)
Si	+1.1, +0.725 ^a	4.15	0.093
O (bulk)	-0.55	3.47	0.054
O (silcanol)	-0.675, -0.9 ^a	3.47	0.122
H	+0.4	1.085	0.015
Na ⁺	+1.0	3.17	0.094

^aSodium siloxide groups require +0.725e for Si and -0.9e for O.

^b r_{ii} is the distance at which the potential reaches its minimum.

Models of Q3/Q4 surfaces with ~ 4.7 silanol groups per nm^2 were obtained by cleavage of the $(10\bar{1})$ plane of α -cristobalite and the hydration of dissociated bonds to silanol groups following Heinz group's work⁴. Silica surface with various pH were obtained by deletion of hydrogen atoms from $\equiv\text{Si-OH}$ groups (silanol groups) and addition of sodium ions to create $\equiv\text{SiO}^-\text{Na}^+$ groups (siloxide groups).

For all 6 systems, 100ps water equilibration at 300K was performed after 1000 steps of water minimization. The whole system containing silica surface, protein, water and ions was then heated up to 300 K at a rate of 0.1 ps/K followed by the equilibration for 270 ps. The production simulation was pursued for 100 ns at 300 K in NVT ensemble. Structural and thermodynamic properties were recorded for the last 10 ns of the trajectory. Silicon and oxygen of silica slab were fixed throughout the simulation, only protein, water and ions were flexible, the integration timestep was 1 fs, the SHAKE algorithm and PBC were used. The cutoff for van-der-Waals interactions was

12 Å, and the smooth particle mesh Ewald (SPME) summation^{6,7} with PME grid spacing ratio of 1 was used for the long-range Coulomb interaction.

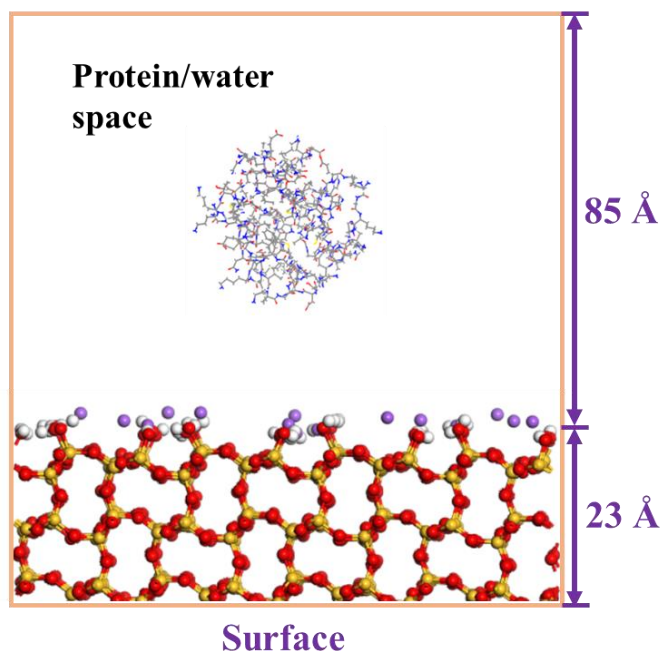


Figure S5. Illustration of periodic simulation box and silica structures used in this study, silicon is yellow, oxygen is red, hydrogen is white and sodium ion is purple.

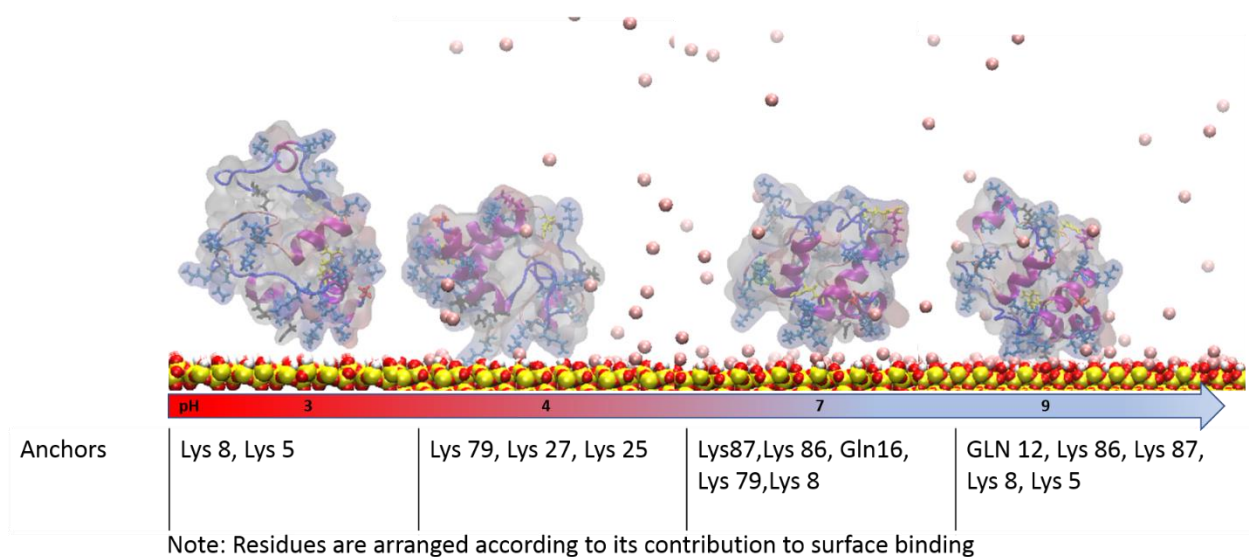


Figure S6. Equilibrium adsorption state of cytochrome c on SiNP41 surface at increasing pH. SiO₂ are shown in VdW spheres where silicon is yellow, oxygen is red, hydrogen is white and sodium ions are pink. Protein surface colored by residue type is shown as a ghost surface. The secondary structure is shown by cartoon and colored as follows: purple, α -helix; lime, 310 helix; red, pi-helix; blue, extended β -sheet; cyan, bridged β -sheet; pink, β -turns. N-ter is indicated by red licorice, and C-ter is colored by purple licorice. Lys, Arg and Gln residues are colored by cerulean, yellow and black, respectively.

V. Instrumental details SANS

The SANS data presented in this paper were collected at two different neutron sources. The data for native cytochrome *c* and the 41 nm silica particles with adsorbed cytochrome *c* were collected at instrument PAXY at the Laboratoire Léon Brillouin (LLB) in Saclay (France). The data for the 7 nm and 13 nm silica particles with adsorbed cytochrome *c* were obtained at instrument KWS 1 at the Forschungsreaktor München II (FRM II) neutron source in Garching, Germany. Experimental details on the instrumental setups used at the two instruments are summarized in Table S7.

Table S7. Instrument setup of the two SANS instruments used in the present experiments

	Setup	K1	K2	K3
Paxy	Wavelength λ / nm	5.00	5.00	17.00
	Collimation length / m	*)	*)	*)
	Detector distance / m	1.1	5.0	5.0
	Beam size / mm ²	10 × 10	10 × 10	10 × 10
KWS 1	Wavelength λ / nm	4.50	4.50	4.50
	Collimation length / m	8.0	20.0	20.0
	Detector distance / m	2.0	4.0	20.0
	Beam size / mm ²	30 × 30	30 × 30	30 × 30

*) At this instrument the collimation length was automatically optimized according to the sample/detector distance.

References

- (1) Bharti, B.; Meissner, J.; Findenegg, G. H. Aggregation of Silica Nanoparticles Directed by Adsorption of Lysozyme. *Langmuir* **2011**, *27*, 9823–9833.
- (2) Larson-Smith, K.; Jackson, A.; Pozzo, D. C. Small Angle Scattering Model for Pickering Emulsions and Raspberry Particles. *J. Colloid Interface Sci.* **2010**, *343*, 36–41.
- (3) Meissner, J.; Prause, A.; Bharti, B.; Findenegg, G. H. Characterization of Protein Adsorption onto Silica Nanoparticles: Influence of PH and Ionic Strength. *Colloid Polym. Sci.* **2015**, *293*, 3381–3391.
- (4) Emami, F. S.; Puddu, V.; Berry, R. J.; Varshney, V.; Patwardhan, S. V.; Perry, C. C.; Heinz, H. Force Field and a Surface Model Database for Silica to Simulate Interfacial Properties in Atomic Resolution. *Chem. Mater.* **2014**, *26*, 2647–2658.
- (5) Banci, L.; Bertini, I.; Huber, J. G.; Spyroulias, G. a; Turano, P. Solution Structure of Reduced Horse Heart Cytochrome C. *J. Biol. Inorg. Chem.* **1999**, *4*, 21–31.
- (6) Essmann, U.; Perera, L.; Berkowitz, M. L.; Darden, T.; Lee, H.; Pedersen, L. G. A Smooth Particle Mesh Ewald Method. *J. Chem. Phys.* **1995**, *103*, 8577–8593.
- (7) Kastenholz, M. A.; Hünenberger, P. H. Influence of Artificial Periodicity and Ionic Strength in Molecular Dynamics Simulations of Charged Biomolecules Employing Lattice-Sum Methods. *J. Phys. Chem. B* **2004**, *108*, 774–788.